Close sequence comparisons are sufficient to identify human *cis*-regulatory elements

Shyam Prabhakar[1,2*], Francis Poulin[1^], Malak Shoukry[1], Veena Afzal[1], Edward M. Rubin[1,2], Olivier Couronne[1,2] and Len A. Pennacchio[1,2*]

[1] Genomics Division, Lawrence Berkeley National Laboratory, Berkeley, California 94720 USA.

[2] U.S. Department of Energy Joint Genome Institute, Walnut Creek, California 94598 USA.

[^] Present address: Department of Integrative Biology, University of California, Berkeley, Berkeley, CA 94720

[*] To whom correspondence should be addressed:

Email: SPrabhakar@lbl.gov, LAPennacchio@lbl.gov

Phone: (510) 495-2853, (510) 486-7498

Running title: Close comparisons detect human regulatory elements

Keywords: Comparative genomics, transcriptional enhancer, *cis*-regulatory, conserved noncoding sequence.

Abstract

Cross-species DNA sequence comparison is the primary method used to identify functional noncoding elements in human and other large genomes. However, little is known about the relative merits of evolutionarily close and distant sequence comparisons. To address this problem, we identified evolutionarily conserved noncoding regions in primate, mammalian and more distant comparisons using a uniform approach (Gumby) that facilitates unbiased assessment of the impact of evolutionary distance on predictive power. We benchmarked computational predictions against previously identified *cis*-regulatory elements at diverse genomic loci, and also tested numerous extremely conserved human-rodent sequences for transcriptional enhancer activity using an *in vivo* enhancer assay in transgenic mice. Human regulatory elements were identified with acceptable sensitivity (53-80%) and true-positive rate (27-67%) by comparison with 1-5 other eutherian mammals or 6 other simian primates. More distant comparisons (marsupial, avian, amphibian and fish) failed to identify many of the empirically defined functional noncoding elements. Our results highlight the practical utility of close sequence comparisons, and the loss of sensitivity entailed by more distant comparisons. We derived an intuitive relationship between ancient and recent noncoding sequence conservation from whole-genome comparative analysis that explains most of the observations from empirical benchmarking. Lastly, we determined that, in addition to strength of conservation, genomic location and/or density of surrounding conserved elements must also be considered in selecting candidate enhancers for *in vivo* testing at embryonic time points.

Introduction

The majority of long-range *cis*-regulatory elements in the human genome have yet to be identified. These gene regulatory modules, which likely number in the tens or hundreds of thousands, are hard to detect, since they lack any obvious distinguishing features analogous to codon structure, splicing motifs, open reading frames, or other hallmarks of protein-coding genes. Furthermore, functional sequences of this class are mostly unique in the genome (Bejerano et al. 2004a), which largely rules out paralogy-based identification. The possibility that regulatory elements could lie more than 1 Mb from their target genes (Lettice et al. 2003; Nobrega et al. 2003) presents another challenge. Consequently, cross-species sequence comparisons, which rely upon the slow substitution rate of many categories of functional DNA relative to neutral sequence, have emerged as the preeminent means of identifying candidate *cis*-regulatory elements in large genomes such as human (Ahituv et al. 2004; Chapman et al. 2004; de la Calle-Mustienes et al. 2005; Hughes et al. 2005; King et al. 2005; Nobrega et al. 2003; Pennacchio and Rubin 2001; Woolfe et al. 2005).

Distant comparisons, such as human-fugu (Brenner et al. 1993; de la Calle-Mustienes et al. 2005; Nobrega et al. 2003; Woolfe et al. 2005), have proven especially powerful at high-specificity prediction of functional elements, since neutral sequences have had sufficient time to diverge beyond recognition. However, despite the similar gene content of the human and fugu genomes, even functional noncoding elements are likely to have diverged over such great distances, as demonstrated by the small number (thousands) of

human-fugu conserved noncoding sequences (CNSs) in the genome. At the other extreme, primate sequence comparisons (Boffelli et al. 2003) are likely to capture most functional components of the human genome due to shared biology, but suffer from low resolution due to insufficient neutral divergence among primate taxa (Eddy 2005). Mammalian genome comparisons have been proposed as a compromise between the requirements of sequence divergence and biological similarity (Cooper et al. 2003), and efforts are under way to sequence 16 additional mammalian genomes, albeit at low coverage (Margulies et al. 2005).

Here, we present an empirical and genomic evaluation of the relative merits of close and distant sequence comparisons at detecting functional noncoding regions in the human genome. Our study complements recent theoretical analyses of this problem (Eddy 2005, Stone et al. 2005) and is directly relevant to the choice of species for whole-genome sequencing and comparative analysis. Additionally, given that regulatory divergence is often proposed as a primary mechanism of phenotypic variation, it is important to characterize the rate of decline of noncoding sequence conservation with increasing evolutionary distance. To impartially assess the effect of evolutionary distance on the predictive power of noncoding conservation, we used a uniform computational approach (Gumby) to detect CNSs in primate, mammalian and more distant sequence alignments. Close and distant comparisons were tested at three diverse genomic loci, for which numerous *cis*-regulatory elements have been characterized experimentally. To complement these empirical results, we performed a whole-genome meta-analysis of human-rodent, human-mouse-chicken, human-mouse-frog and human-mouse-fish whole-

genome CNS sets, and uncovered a general principle linking shallow and deep evolutionary constraint. Finally, we performed systematic *in vivo* testing of extremely conserved human-rodent CNSs in an *in vivo* transgenic mouse enhancer assay and identified with high specificity developmental enhancers missed by human-fish comparative analysis, and in the process determined that genomic context is a critical factor in identifying such enhancers.

Results

Assessment of Whole-Genome Noncoding Conservation among Mammals and more Distant Species

Coding exons are known to retain sequence similarity across great evolutionary distances, such as that between human and pufferfish (Aparicio et al. 2002). In contrast, intronic and intergenic conserved elements "evaporate" much more rapidly, thus limiting the sensitivity of distant noncoding sequence comparisons. To quantify the decay of noncoding sequence conservation with evolutionary distance, we generated whole-genome CNS sets through Gumby analysis (see Methods) of the following three-way genome alignments: human-mouse-rat (HMR), human-mouse-chicken (HMG), human-mouse-frog (HMX), and human-mouse-fish (HMF; see Methods). In the human-rodent alignment, we identified 171,853 CNSs representing 2.2% of the human genome (Gumby *P*-value $\leq$ 1e-3). At the same *P*-value threshold, the corresponding CNS statistics were 40,033 and 0.37% for human-mouse-chicken, 14,568 and 0.13% for human-mouse-frog, and 5,668 and 0.044% for human-mouse-fish. As expected, the more distantly related genomes exhibit markedly less conservation relative to human, suggesting a reduction in sensitivity that offsets their increased specificity in detecting functional noncoding regions.

In order to correlate mammalian and more ancient noncoding conservation, we classified whole-genome CNSs into 4 primary categories. Category 1 consists of human-rodent

CNSs that overlap human-mouse-chicken, human-mouse-frog and human-mouse-fish CNSs. Category 2 extends only to human-mouse-frog, Category 3 to human-mouse-chicken, and Category 4 is restricted to human-rodent alone. Median length and -log(*P*-value) of CNSs within a given category and phylogenetic scope (for instance, Category 2 and human-mouse-frog) were represented by the dimensions of a single rectangular block. Building on such blocks, we define shapes generated by stacking blocks of the same category as Evolutionary Stacking Patterns (ESPs, Figs. 1A-D). Although there is considerable variation within each category, the 4 ESPs characterizing the 4 CNS categories illustrate two general trends: 1) CNSs shrink as evolutionary distance increases, with the tallest stacking pattern tapering from 712 bp at its phylogenetically "shallow" end (human-rodent) to 228 bp at its "deep" end (human-mouse-fish). 2) Close-species CNSs are longer and have stronger *P*-values when they are also conserved in distant species. For example, while human-rodent CNSs conserved in chicken, frog and fish have median length 712 bp and *P*-value 4.1e-35, human-rodent CNSs with no significant non-mammalian conservation have median length 268 bp and *P*-value 2.2e-06. Since they arise from the characteristic funnel shape of ESPs, we refer to these two trends collectively as the "funnel principle" of noncoding conservation.

The funnel principle suggests that highly conserved human-rodent CNSs should be enriched for conservation in non-mammals. To quantify this enrichment, we sorted whole-genome human-rodent CNSs by *P*-value, and calculated the fraction of human-mouse-chicken, human-mouse-frog and human-mouse-fish CNSs overlapped by various quantiles of the human-rodent set (Fig. 2A). Remarkably, we see that the top 10% of the

human-rodent CNSs overlap 60% of the CNSs in the human-mouse-fish set, 46% of the human-mouse-frog set and 30% of the human-mouse-chicken set, indicating that a large fraction of deeply conserved CNSs can paradoxically be identified through shallow evolutionary comparisons. Similarly, almost half (47%) of the human-mouse-fish CNSs are contained in the top 5% of the human-rodent set. In terms of probabilities, the highest-scoring human-rodent CNSs have an 86% chance of being significantly conserved in chicken, while the lowest-scoring ones have less than a 4% chance of being in the human-mouse-chicken set (Fig. 2B). The corresponding likelihoods are 81% and 0.75% in human-mouse-frog, and 64% and 0.2% in human-mouse-fish (see Supplementary Methods for analyses of potential artifacts).

Although we see a significant correlation between ancient and recent noncoding conservation, there are also important differences between the two phenomena. While half (2,834) of the whole-genome human-mouse-fish CNSs have a human-rodent *P*-value < 1.9e-28, there are 7,686 human-rodent CNSs that meet the same *P*-value criterion, and yet lack significant conservation in fish. These data indicate that human-rodent analysis is capable of identifying a much larger set of unambiguously constrained noncoding elements than are obtainable from mammal-fish comparison.

It is conceivable that the funnel principle could merely reflect biases in the algorithm used to identify CNSs, as would indeed be the case if close and distant comparisons were not performed uniformly, or if the CNS sets were corrupted with significant numbers of false-positive predictions. We therefore performed evolutionary simulations and further

statistical analyses, which confirmed that such artifacts are unlikely (see Supplementary Methods).

In Vivo Experimental Validation and Assessment: Four Human-Genome Loci

I. *DACH1*: *in vivo* testing of the top-scoring human-rodent conserved elements

In order to empirically evaluate the power of extreme human-rodent conservation to identify developmental enhancers, we analyzed the locus of *DACH1,* a transcription-cofactor gene involved in limb, eye and brain development (Davis et al. 1999). The 2-Mb genomic region containing *DACH1* and most of its flanking intergenic DNA (human chr13:70,207,792-72,205,000; NCBI Build 35) contains 1,084 human-mouse CNSs by the standard criterion of 70% sequence identity over 100 bp, thus necessitating some criterion for prioritizing the abundance of human-rodent elements. It has previously been demonstrated that human-fish conservation constitutes one such criterion for prioritizing human-rodent elements, in that restricting the analysis to human-fish CNSs facilitated the identification of transcriptional enhancers with a high true-positive rate (Nobrega et al. 2003). In the present study, we attempted to achieve a comparable true-positive rate and yet greater sensitivity by focusing instead on the human-rodent CNSs with the most extreme (*i.e.* very low) *P*-values.

We first assessed the overlap between the most conserved human-rodent CNSs and human-fish CNSs in the *DACH1* locus. Consistent with the above-described funnel principle, we found that 22 of the 36 strongest human-mouse-rat CNSs in this locus (P-

value ≤ 1e-50) are conserved in at least one of the three available fish genomes. These 22 include 5 of the 7 human-fish CNSs previously validated through *in vivo* enhancer testing (Nobrega et al. 2003). Thus, in addition to having a high likelihood of ancient conservation in distant species, the 36 human-rodent CNSs with extreme *P*-values are also enriched for known developmental enhancers, relative to the entire set of 1,084 human-mouse CNSs in the vicinity of *DACH1*.

To demonstrate the independent predictive power of extreme human-rodent conservation, we focused on the 14 CNSs within the aforementioned set of 36 that exhibited no conservation in fish, and randomly selected 6 of them to assay for transcriptional enhancer activity *in vivo*. Our assay fuses the human conserved element to a beta-galactosidase reporter vector and assesses the ability of the conserved fragment to drive tissue-specific expression in transgenic mice at embryonic day 11.5-12.5 (e11.5-12.5) (Kothary et al. 1989)(see Supplementary Methods). For 3 of the 6 extreme human-rodent elements tested, we found reproducible beta-galactosidase expression localized to the limbs, eyes and forebrain, consistent with aspects of the endogenous developmental expression pattern of *DACH1* (Caubit et al. 1999; Davis et al. 1999) (Fig. 3). Beta-galactosidase expression was not reproducibly localized to any other anatomical structure of the embryos.

To test the predictive power of human-rodent conservation *P*-values on a larger scale, we retrospectively analyzed 133 human-fugu and ultra-conserved (Bejerano et al. 2004b) CNSs that were tested for *in vivo* enhancer function as part of a separate whole-genome

survey (Pennacchio et al. 2006). Each of the 133 CNSs was assigned a Gumby human-rodent conservation score (-log(*P*-value)). We found that positive enhancers had significantly higher conservation scores than negatives (t-test *P*-value=0.0001), which further confirms the validity of using human-rodent *P*-values to prioritize candidate embryonic enhancers.

II. Human chromosome 16: genomic distribution of enhancers active at embryonic day 11.5-12.5

Though reliable indicators of function, human-fish CNSs tend to be limited in number and strongly clustered in genomic regions containing a handful of developmental genes and transcription factors (Sandelin et al. 2004; Woolfe et al. 2005). For example, the human-mouse-fish CNSs on human chromosome 16 are highly skewed towards four gene-poor loci (Fig. 4) containing the developmentally regulated genes *SALL1*, *IRX3*, *IRX5*, *IRX6*, *ATBF1* and *WWOX*. The density graph of human-rodent CNSs on this chromosome displays peaks at the same locations as human-mouse-fish, and also additional peaks absent in human-mouse-fish. On the basis of positive results from the *DACH1* pilot study, we hypothesized that human-rodent CNSs with extreme *P*-values could also identify developmental transcriptional enhancers in these additional loci, to compensate for their poor coverage by human-mouse-fish CNSs.

To test this hypothesis, we focused on the 50 top-scoring "non-fish" human-mouse-rat CNSs on chromosome 16 (*P*-value < 1e-40), of which 36 were located outside the four developmental loci encompassed by human-mouse-fish conservation. We tested 11 of

these 36 for *in vivo* enhancer function through our mouse enhancer transgenesis assay and found to our surprise that not a single one of these 11 CNSs drove a reproducible embryonic expression pattern, in contrast to our experience at the *DACH1* locus. It is possible that these CNSs are not transcriptional enhancers despite extreme human-rodent conservation, or that their activities are beyond the resolution/sensitivity of this assay or perhaps even that they are enhancers at a different embryonic time point.

To determine if extreme human-mouse-rat CNSs are better able to capture transcriptional enhancers flanking key developmental transcription factor and signaling genes, we tested 13 of the 14 extreme human-rodent CNSs (*P*-value <1e-40) that lie within the 4 gene-poor regions on chromosome 16 containing the aforementioned developmental genes. Of these 13 CNSs, 5 (38%) drove reproducible beta-galactosidase gene expression, a success rate comparable to the rate of 41% observed in systematic tests of human-fish CNSs on the same chromosome (L. Pennacchio, unpublished data; http://enhancer.lbl.gov/). The disparity in success rate among different loci on chromosome 16 suggests that genomic context must be considered in addition to conservation score in selecting candidate enhancers for testing at this embryonic time point.

III. SCL Benchmark: Benefits of Multiple-Eutherian Comparison

The human Stem Cell Leukemia (SCL) locus provides an excellent benchmark for evaluating the effect of phylogenetic scope on comparative sequence analysis, based on the detailed experimental definition of 9 non-exonic murine DnaseI-hypersensitive sites (DHSs) and one additional enhancer in the genomic region containing the SCL gene and

its flanking intergenic segments (Chapman et al. 2004). Weak homology to chicken has been reported (Gottgens et al. 2000) for a subset of these functional elements in alignments generated using DIALIGN (Brudno et al. 2003a). However, with the exception of one of the SCL promoters, none of the 10 experimentally defined elements shows significant conservation in LAGAN alignments to non-mammalian species such as chicken, frog, fugu, tetraodon or zebrafish, exemplifying the loss of sensitivity entailed by distant sequence comparisons (data not shown).

Given the poor sensitivity of distant sequence comparisons, we aligned the available human, mouse, rat and dog sequences from this locus (human chr1:47,367,748-47,427,851; NCBI Build 35) using MLAGAN, which yielded a total divergence of 0.79 substitutions/site. At the default *P*-value threshold of 0.5, Gumby conservation analysis (see Supplementary Methods) detected 8 of the 10 experimentally defined noncoding elements, with 11 new predictions (Fig. 5). Thus, as in the case of *DACH1, P*-value prioritization of CNSs in just a few eutherian genomes is sufficient to identify with acceptable true-positive rate functional elements missed by distant sequence comparison. Of the 8 functional regions detected by human-mouse-rat-dog analysis, 7 have *P*-value $\leq$ 1.3e-4, whereas only one of the new predictions meets the same criterion, suggesting that most of the known functional elements in this region are clearly distinguishable from neutrally evolving DNA. Indeed, when we reduced the statistical power of the sequence comparison by restricting our analysis to human and mouse alone, (branch length 0.47 substitutions/site), Gumby still identified only one new prediction within the *P*-value range of the 7 prominent benchmark elements. Remarkably, even mouse-rat pairwise

comparison (*P*-value ≤ 0.5) succeeded in identifying 6 of the benchmark elements with only 3 new predictions, despite the minimal neutral divergence (0.14 substitutions/site) between the two rodents. These results demonstrate that very low levels of neutral sequence divergence are sufficient for identification of well-conserved enhancers and DHSs, though functional elements marked by marginal levels of sequence conservation are better detected when total branch length is augmented by introduction of additional eutherians to the species set.

IV. Alpha-Globin Benchmark: Simians, Primates, Mammals

The human alpha-globin locus is another well-characterized genomic region, with a recent synthesis of extensive computational and empirical analyses cataloging 17 functional noncoding DNA elements (Hughes et al. 2005). The elements comprise 11 promoters, 4 non-promoter DHSs involved in transcriptional regulation, and 2 putative regulators of alternative splicing. In addition, this locus is well suited to evaluating the relative merits of close and distant sequence comparisons, due to the availability of sequence data from 22 vertebrate species spanning a broad range of evolutionary distances from old world monkeys to teleost fish. The analyzed genomic region (human chr16:48339-219839; NCBI Build 35) spans the block of conserved synteny telomeric to the alpha-globin genes, the alpha-globin genes themselves, and the *LUC7L* gene. To ensure accurate alignment, we split the locus into four subregions, and aligned each subregion separately (see Supplementary Methods).

As was the case with the SCL locus, conservation of the benchmark functional elements

in distant species is extremely limited; frog and fish have no apparent sequence homology to any of the 17 noncoding functional elements, and chicken shows homology to only 2 of the 17. Sequence conservation is also limited in opossum, and even hedgehog (which is the most diverged of the eutherians considered here) shows no similarity for 5 of the 17 benchmark sequence elements (see (Hughes et al. 2005) for a detailed breakdown of conservation by species).

To assess the relative power of various eutherian comparisons at this locus, we selected the following three species sets: (1) Simians (human, baboon, colobus, squirrel monkey, owl monkey, marmoset, dusky titi), (2) Primates (simian group plus the prosimian galago), and (3) Eutherians minus non-human primates and hedgehog (human, mouse, rat, cat, cow, pig). In the eutherian set, which had a total branch length ranging from 1.24 to 1.55 substitutions/site across the 4 sub-regions, Gumby identified 13/17 benchmark elements, with 22 new predictions (P-value ≤ 0.5). Primate and simian comparisons were performed with P-value thresholds adjusted to yield the same number of new predictions (22) as in the eutherian comparison, so as to fairly assess relative sensitivity of the three species sets. The resulting sensitivity of the primate comparison (0.45-0.69 substitutions/site) was 11/17, while the simian comparison (0.25-0.39 substitutions/site) had a sensitivity of 9/17, demonstrating that predictive power declines as evolutionary divergence decreases in closely-related species. Although the simian comparison displayed the lowest statistical power, it is notable that a sensitivity of 53% (9/17) and a true positive rate of at least 29% (9/(9 + 22)) were achieved by comparing no more than 6 simian genomes to human in any of the four sub-regions.

Discussion

Ancient human-fish noncoding conservation has been the mainstay of searches for enhancers of key developmental genes, whereas mammalian sequence comparisons have been considered insufficiently specific, especially in large, highly conserved intergenic regions harboring hundreds of human-rodent CNSs. This dichotomy disappears in light of the funnel principle established by whole-genome meta-analysis of close and distant sequence comparisons: the longer and more constrained a mammalian CNS, the deeper its evolutionary conservation in distant vertebrates (on average), and *vice versa*. Thus, extreme human-rodent *P*-values serve as a proxy for human-fish conservation, and most human-fish CNSs can be identified through human-rodent analysis alone. The correspondence between recent and ancient sequence conservation is likely to grow even stronger when more mammalian genomes are added to the human-mouse-rat trio (Margulies et al. 2005). A relationship between ancient and recent noncoding conservation consistent with the funnel principle has been reported earlier (Ovcharenko et al. 2004), though the correspondence described between the two evolutionary scales was significantly weaker than is evident from our results. Although human-fish sequence comparison identifies developmental enhancers with high specificity, only a small fraction of the expected tens or hundreds of thousands of functional noncoding elements in the human genome are conserved in fish. Extreme-*P*-value mammalian CNSs form a superset covering the majority of human-fish as well as a much larger fraction of noncoding functional elements in the human genome, while still maintaining a low false-positive rate. More generally, in identifying candidates for experimental testing, the

tradeoff between sensitivity and specificity can be tuned simply by adjusting the threshold conservation score (*P*-value), in contrast to the more common technique of varying the evolutionary distance between the compared species.

In vivo assays of 30 extreme human-rodent CNSs with no conservation in fish yielded 8 positive enhancers at e11.5-12.5, close to the success rate of human-fish comparison. This experimentally confirms the theoretical prediction that extreme conservation in relatively close species is on par with conservation between highly diverged species. In terms of genomic distribution, the success rate was 8/19 among human-rodent CNSs in the neighborhood of developmental genes such as *DACH1*, *SALL1*, *IRX3*, *IRX5*, *IRX6*, *ATBF1* and *WWOX*, and it was 0/11 at other loci on human chromosome 16, most likely since the assay is limited to gene with complex tissue-specific expression at e11.5/12.5, and produces false negatives in loci that are silent or regulated in relatively simple manner at this embryonic time point. Since such *in vivo* tests are expensive and time-consuming, one strategy for large-scale functional genomics would be to prioritize loci that are known to require tissue-specific regulation at the selected developmental stage. Alternatively, one could prioritize loci of unknown function that nevertheless have a high density of ancient (human-mouse-fish, or perhaps even human-mouse-frog or human-mouse-chicken) CNSs, since the loci on human chromosome 16 yielding high success rates in the embryonic enhancer assay were originally identified solely on the basis of their high human-mouse-fish CNS density (Fig. 4). For instance, the second-largest peak of human-mouse-fish CNS density in the human genome (data not shown) occurs between the first exons of the uncharacterized human genes *ZNF503* and *C10orf11*,

making these genes candidates for deeply conserved and highly specific early developmental regulation.

Results from whole-genome conservation analysis, from benchmarking using pre-existing functional datasets from three diverse genomic loci and from systematic *in vivo* characterization of 30 new enhancer predictions, all indicate the considerable statistical power of sequence comparisons involving just a few (3-6) eutherian mammals. Another consistent theme is the loss of sensitivity when more distant species such as marsupials, chicken, frog and fish are compared to human, either because they have diverged in their *cis*-regulatory programs, or because of stabilizing selection that allows the regulatory sequence to diverge while retaining the same tissue and temporal specificity (Ludwig et al. 2000; Oda-Ishii et al. 2005). At the other extreme, simian sequence comparisons in the alpha-globin locus performed surprisingly well despite their low total divergence (0.25-0.39 substitutions/site), achieving a sensitivity of 53% and a true positive rate of at least 29%. The funnel principle provides one possible explanation: since the length of a CNS in human-mouse-chicken is on average greater than that of its equivalent in human-mouse-fish, and the corresponding mammalian CNS is longer still, the size of constrained blocks in simians should by extrapolation be greater than that in mammals, thus offering simian comparisons a larger target, and partially compensating for their lower neutral divergence.

It is common in analyses of the statistical power of sequence comparisons to fix the size of an individual constrained block as total branch length (neutral divergence) is varied

(Eddy 2005; Margulies et al. 2003; Stone et al. 2005). However, the funnel principle implies that the two variables are not independent, and that constrained blocks shrink when more distant species are compared. Thus, for a given total branch length, one could maximize block size, and consequently statistical power, by choosing multiple extremely close species (say, simian primates) over a few more diverged species (mammals).

In this study, we have focused on the identification of large sequence elements with empirical evidence of *cis*-regulatory function, such as enhancers, promoters and DnaseI-hypersensitive sites, which have typical lengths of 100 bp or more. Previous theoretical studies (Cooper et al. 2005; Eddy 2005) have shown that higher-resolution functional prediction at the level of a transcription-factor binding site (6-12 bp), or even a single basepair, is likely to require sequence from more than ten mammals spread across the clade. However, a more accessible initial strategy might be to use the existing mammalian genome sequences for prediction of larger, higher-level functional elements, many of which show little or no sequence conservation in distant species. It should also be possible to use sequence data from multiple primates to identify distant regulatory elements that evolve too rapidly to be detected in mammalian sequence comparisons. We have demonstrated that such strategies are highly effective, based on systematic benchmarking of sequence comparisons across a broad range of phylogenetic scopes against empirical data from a diverse array of genomic loci. While the sequencing of additional mammalian genomes will incrementally facilitate identification of large regulatory modules in the human genome, it is likely that the greatest strength of deep mammalian genomic alignments will be in computationally dissecting their internal

structure.

Methods

Development of a Uniform Statistical Scoring Scheme for Sequence Conservation (Gumby)

In order to uniformly evaluate the benefits and limitations of close versus distant sequence comparisons, we sought a computational algorithm general enough to process alignments at all evolutionary distances, identify conserved regions of any size, and most importantly quantify their statistical significance (*P*-value). For generality and convenience, we further stipulated that the method should require no training data, no prior estimates of evolutionary rates (branch lengths), and only one arbitrary parameter, which could remain fixed across all evolutionary distances. The Gumby program meets these design goals by making minimal assumptions about the statistical features of conserved noncoding regions, and treating the sequence alignment as its own training set. Gumby takes its name from the Gumbel distribution, which is the extreme value distribution underlying Karlin-Altschul statistics. The input data are an alignment, a phylogenetic tree (topology only, without branch lengths), and annotations of coding regions (optional). The algorithm proceeds through five steps:

(1) Noncoding regions in the input alignment are used to estimate the neutral mismatch frequency p_N between each pair of aligned sequences. This is done simply by counting the number of mismatches in nonexonic positions, and dividing by the number of aligned nonexonic positions. Failure to provide exon annotations introduces a bias in the

mismatch frequency that is proportional to the fraction of genomic DNA contained in exons, which is generally small in vertebrates.

(2) A log-odds scoring scheme for constrained versus neutral evolution is then independently initialized for each pair of sequences, based on the assumption that the mismatch frequency p_C in constrained regions equals p_N/R, where the ratio R is an arbitrary parameter. For example, if R = 3/2 (default value), constrained regions are expected to evolve at 2/3 times the neutral rate, until sequence divergence begins to saturate. The log-odds mismatch score for the sequence pair is then given by $S_0 = \log((p_N/R) / p_N) = -\log(R)$, and the match score is $S_1 = \log((1 - p_N/R) / (1 - p_N))$. The default R-ratio (1.5) was selected to optimize the sensitivity-specificity tradeoff in detecting empirically defined regulatory elements in the *SCL* locus (Supplementary Figure 1). However, other values of R gave very similar results, perhaps because 7 of the 10 benchmark regulatory elements are very significantly conserved, and therefore robustly distinguishable from the rest of the locus. Gap characters in the alignment are assigned a weighted average of mismatch and match scores: $S_G = p_N S_0 + (1 - p_N) S_1$. This gap score is guaranteed to be negative, and has the effect of lightly penalizing indels; a compromise between treating them as mismatches, which is the usual practice for algorithms implementing phylogenetic "shadowing", and ignoring them altogether, as is common when the species set is sufficiently diverged. Missing data, i.e. "N" nucleotides, are given a zero score. However, one drawback of any scoring scheme that penalizes gaps is that failure to flag sequencing gaps with "N" characters results in spurious alignment gaps, which artificially lower the conservation score of the corresponding region in the

alignment.

(3) Each alignment column is scored as a sum of pair-wise log-odds scores along a circular tour of the phylogenetic tree. For example, for the phylogenetic tree shown in Supplementary Figure 2, the circular-tour column score is S = S(human,mouse) + S(mouse,cow) + S(cow,dog) + S(dog,lemur) + S(lemur,human). This averaging scheme traverses each branch in the phylogenetic tree the same number of times, and thus permits simple phylogenetic scoring of multiple alignments while avoiding the drawbacks of sum-of-pairs and consensus schemes. The resulting conservation score fulfills the requirements of Karlin-Altschul statistics, in that positive column scores are possible, though the average column score is negative (Karlin and Altschul 1990).

(4) Conserved regions appear as stretches of alignment columns with a high aggregate score. Gumby traverses the alignment from left to right, initiating a conserved segment at each new alignment column with a positive score, and extending the segment until the aggregate score becomes negative, at which point the right edge of the segment is retraced to the alignment column yielding the maximal aggregate segment score. This procedure guarantees that both boundaries of each segment are maximal with respect to segment score, thus eliminating the need for setting arbitrary window sizes, and allowing detection of long, weakly conserved regions as well as short, strongly conserved elements. This feature is also important in achieving generality across close and distant sequence comparisons, since short conserved elements are not likely to be statistically significant in sequence comparisons with low total neutral divergence (for example,

primate shadowing).

(5) The aggregate score of the alignment columns in each conserved region is translated into a *P*-value using Karlin-Altschul statistics. As is the case with the BLAST algorithm (Altschul et al. 1990), the *P*-value of a given conserved element varies with the size of the search space, since one is more likely to find a given degree of conservation by random chance in a long alignment than in a short alignment. To make the *P*-values comparable across alignments of different lengths, Gumby normalizes them to refer to a fictitious fixed-length alignment with the same statistical properties as the true alignment. In other words, the *P*-value answers the question, "What is the likelihood of seeing such a high conservation score in a pseudo-alignment of length 10 kb that is generated by randomly selecting columns from the given alignment?" The 10-kb *P*-value is related to the expected number of false positives in a 10-kb region (i.e. the 10-kb *E*-value) as follows: $P = 1 - \exp(-E)$. When $P << 1$, $P \approx E$. Thus, the *P*-value also doubles as an estimate of the false-positive rate.

One pitfall in applying Karlin-Altschul statistics to global alignments is the fact that column scores are not identically distributed. For example, the distribution of scores at positions that are aligned in, say, 5 of 10 species is different from that at positions that are unique to a single species. Also, the number of aligned species is highly correlated between neighboring alignment columns, due to the block-like structure generated by long indels. The fictitious randomly permuted alignments modeled by Karlin-Altschul statistics do not have this correlation structure, and are therefore less likely to contain

local high-scoring segments than are neutral regions in real alignments. Thus, a straightforward application of the permutation-based null model generates unrealistically strong *P*-values. To compensate for this effect, Gumby takes the conservative approach of estimating the Karlin-Altschul K and λ parameters only on the basis of columns that are aligned in at least *k* species (*k* >= 2). As *k* is increased, the number of columns in the null model decreases. Gumby sets *k* to the maximum value such that the number of columns in the null model is at least 40% of the length of the base sequence. Another source of spurious *P*-values is the suppression of null-model scores by large indels that are artifacts of missing sequence data. Gumby again takes the conservative approach of penalizing indels only after the null model has been generated.

Gumby Availability

Gumby conservation analysis is automatically performed when DNA sequences are submitted to the VISTA server (Frazer et al. 2004) (http://genome.lbl.gov/vista), and conserved regions are graphically displayed using RankVISTA. Precomputed whole-genome Gumby results based on pair-wise alignments are available as RankVISTA tracks on the VISTA Browser (http://pipeline.lbl.gov). Gumby source code is available at http://pga.lbl.gov/gumby.

Generation of Whole-Genome CNS Sets

Whole-genome CNS sets were generated as described in (Ahituv et al. 2005). Syntenic

blocks between the compared genomes were defined by PARAGON, globally aligned using MLAGAN (Brudno et al. 2003b), and scanned for statistically significant conserved regions using Gumby. This procedure minimizes false alignments, since only syntenic conservation is allowed. As in previous large-scale analyses (Ahituv et al. 2005), we sought to improve alignment accuracy by performing three-way (human, mouse, non-mammal) instead of pair-wise (human, non-mammal) genome alignments (Brudno et al. 2003b). Consequently, we analyzed alignments between the human and mouse genomes and those of rat (HMR), chicken (HMG), frog (HMX), and fish (HMF; union of human-mouse-fugu, human-mouse-tetraodon and human-mouse-zebrafish). CNSs were defined as conserved regions (*P*-value ≤ 1e-3) that do not overlap known genes, mRNAs or spliced ESTs in any of the aligned genomes. This *P*-value threshold is a factor of 500 below the default threshold of 0.5, and is therefore not suitable for high-sensitivity identification of noncoding regulatory elements. However, it severely limits false-positive predictions, and therefore facilitates reliable characterization of the relations between recent and ancient noncoding conservation.

DACH1 and human chromosome 16: identifying candidate embryonic enhancers

Due to the extreme levels of noncoding constraint observed in the *DACH1* locus, we identified human-mouse-rat CNSs in this genomic region using a Gumby *R*-ratio of 10.0 and a P-value threshold of 1e-50. However, in the larger subsequent analysis of extremely conserved human-mouse-rat CNSs on human chromosome 16, we retained the default R-ratio of 1.5 and relaxed the P-value threshold to 1e-40, so as to obtain a larger

and more representative set of conserved elements. In addition to the aforementioned filters for transcriptional evidence, extreme human-rodent CNSs with more than 40 bp of overlap with human or non-human unspliced ESTs from more than one library were discarded, as were CNSs overlapping single unspliced ESTs with BLASTX matches (Evalue ≤ 0.5) in peptide sequence databases (Altschul et al. 1990). CNSs within 50 bp of exons of known genes were also removed, so as to eliminate potential regulators of pre-mRNA splicing. The remaining human-rodent CNSs were filtered for overlap with Gumby human-mouse-fish CNSs, or with human-fugu, human-tetraodon or human-zebrafish "net" alignments in the UCSC Genome Browser (http://genome.ucsc.edu).

Acknowledgements

We thank Alexander Poliakov and Inna Dubchak for incorporating Gumby into the VISTA web server, Nadav Ahituv for the Gateway-HSP68-LacZ vector, Jim Hughes for feedback regarding alpha-globin sequence analysis, Qian-fei Wang, Jan-Fang Cheng and Michael Brudno for numerous productive conversations during development of Gumby, and James Noonan, Nadav Ahituv, Qian-fei Wang and Dario Boffelli for comments on the manuscript. F.P. was supported by a fellowship from the Canadian Institutes of Health Research. Research was conducted at the E.O. Lawrence Berkeley National Laboratory, supported by the Grant # HL066681, Berkeley-PGA, under the Programs for Genomic Application, funded by National Heart, Lung, and Blood Institute, USA, and performed under Department of Energy Contract DE-AC02-05CH11231, University of California.

References

Ahituv, N., S. Prabhakar, F. Poulin, E.M. Rubin, and O. Couronne. 2005. Mapping cis-regulatory domains in the human genome using multi-species conservation of synteny. *Hum Mol Genet* **14:** 3057-3063.

Ahituv, N., E.M. Rubin, and M.A. Nobrega. 2004. Exploiting human--fish genome comparisons for deciphering gene regulation. *Hum Mol Genet* **13 Spec No 2:** R261-266.

Altschul, S.F., W. Gish, W. Miller, E.W. Myers, and D.J. Lipman. 1990. Basic local alignment search tool. *J Mol Biol* **215:** 403-410.

Aparicio, S., J. Chapman, E. Stupka, N. Putnam, J.M. Chia, P. Dehal, A. Christoffels, S. Rash, S. Hoon, A. Smit, M.D. Gelpke, J. Roach, T. Oh, I.Y. Ho, M. Wong, C. Detter, F. Verhoef, P. Predki, A. Tay, S. Lucas, P. Richardson, S.F. Smith, M.S. Clark, Y.J. Edwards, N. Doggett, A. Zharkikh, S.V. Tavtigian, D. Pruss, M. Barnstead, C. Evans, H. Baden, J. Powell, G. Glusman, L. Rowen, L. Hood, Y.H. Tan, G. Elgar, T. Hawkins, B. Venkatesh, D. Rokhsar, and S. Brenner. 2002. Whole-genome shotgun assembly and analysis of the genome of Fugu rubripes. *Science* **297:** 1301-1310.

Bejerano, G., D. Haussler, and M. Blanchette. 2004a. Into the heart of darkness: large-scale clustering of human non-coding DNA. *Bioinformatics* **20 Suppl 1:** I40-I48.

Bejerano, G., M. Pheasant, I. Makunin, S. Stephen, W.J. Kent, J.S. Mattick, and D. Haussler. 2004b. Ultraconserved elements in the human genome. *Science* **304:** 1321-1325.

Boffelli, D., J. McAuliffe, D. Ovcharenko, K.D. Lewis, I. Ovcharenko, L. Pachter, and E.M. Rubin. 2003. Phylogenetic shadowing of primate sequences to find functional regions of the human genome. *Science* **299:** 1391-1394.

Brenner, S., G. Elgar, R. Sandford, A. Macrae, B. Venkatesh, and S. Aparicio. 1993. Characterization of the pufferfish (Fugu) genome as a compact model vertebrate genome. *Nature* **366:** 265-268.

Brudno, M., M. Chapman, B. Gottgens, S. Batzoglou, and B. Morgenstern. 2003a. Fast and sensitive multiple alignment of large genomic sequences. *BMC Bioinformatics* **4:** 66.

Brudno, M., C.B. Do, G.M. Cooper, M.F. Kim, E. Davydov, E.D. Green, A. Sidow, and S. Batzoglou. 2003b. LAGAN and Multi-LAGAN: efficient tools for large-scale multiple alignment of genomic DNA. *Genome Res* **13:** 721-731.

Caubit, X., R. Thangarajah, T. Theil, J. Wirth, H.G. Nothwang, U. Ruther, and S. Krauss. 1999. Mouse Dac, a novel nuclear factor with homology to Drosophila dachshund shows a dynamic expression in the neural crest, the eye, the neocortex, and the limb bud. *Dev Dyn* **214:** 66-80.

Chapman, M.A., I.J. Donaldson, J. Gilbert, D. Grafham, J. Rogers, A.R. Green, and B. Gottgens. 2004. Analysis of multiple genomic sequence alignments: a web resource, online tools, and lessons learned from analysis of mammalian SCL loci. *Genome Res* **14:** 313-318.

Cooper, G.M., M. Brudno, E.D. Green, S. Batzoglou, and A. Sidow. 2003. Quantitative estimates of sequence divergence for comparative analyses of mammalian genomes. *Genome Res* **13:** 813-820.

Cooper, G.M., E.A. Stone, G. Asimenos, E.D. Green, S. Batzoglou, and A. Sidow. 2005. Distribution and intensity of constraint in mammalian genomic sequence. *Genome Res* **15:** 901-913.

Davis, R.J., W. Shen, T.A. Heanue, and G. Mardon. 1999. Mouse Dach, a homologue of Drosophila dachshund, is expressed in the developing retina, brain and limbs. *Dev Genes Evol* **209:** 526-536.

de la Calle-Mustienes, E., C.G. Feijoo, M. Manzanares, J.J. Tena, E. Rodriguez-Seguel, A. Letizia, M.L. Allende, and J.L. Gomez-Skarmeta. 2005. A functional survey of the enhancer activity of conserved non-coding sequences from vertebrate Iroquois cluster gene deserts. *Genome Res* **15:** 1061-1072.

Eddy, S.R. 2005. A model of the statistical power of comparative genome sequence analysis. *PLoS Biol* **3:** e10.

Frazer, K.A., L. Pachter, A. Poliakov, E.M. Rubin, and I. Dubchak. 2004. VISTA: computational tools for comparative genomics. *Nucleic Acids Res* **32:** W273-279.

Gottgens, B., L.M. Barton, J.G. Gilbert, A.J. Bench, M.J. Sanchez, S. Bahn, S. Mistry, D. Grafham, A. McMurray, M. Vaudin, E. Amaya, D.R. Bentley, A.R. Green, and A.M. Sinclair. 2000. Analysis of vertebrate SCL loci identifies conserved enhancers. *Nat Biotechnol* **18:** 181-186.

Hughes, J.R., J.F. Cheng, N. Ventress, S. Prabhakar, K. Clark, E. Anguita, M. De Gobbi, P. de Jong, E. Rubin, and D.R. Higgs. 2005. Annotation of cis-regulatory elements by identification, subclassification, and functional assessment of multispecies conserved sequences. *Proc Natl Acad Sci U S A* **102:** 9830-9835.

Karlin, S. and S.F. Altschul. 1990. Methods for assessing the statistical significance of molecular sequence features by using general scoring schemes. *Proc Natl Acad Sci U S A* **87:** 2264-2268.

King, D.C., J. Taylor, L. Elnitski, F. Chiaromonte, W. Miller, and R.C. Hardison. 2005. Evaluation of regulatory potential and conservation scores for detecting cis-regulatory modules in aligned mammalian genome sequences. *Genome Res* **15:** 1051-1060.

Kothary, R., S. Clapoff, S. Darling, M.D. Perry, L.A. Moran, and J. Rossant. 1989. Inducible expression of an hsp68-lacZ hybrid gene in transgenic mice. *Development* **105:** 707-714.

Lettice, L.A., S.J. Heaney, L.A. Purdie, L. Li, P. de Beer, B.A. Oostra, D. Goode, G. Elgar, R.E. Hill, E. de Graaff. 2003. A long-range Shh enhancer regulates expression in the developing limb and fin and is associated with preaxial polydactyly. *Hum Mol Genet* **12**:1725-1735.

Ludwig, M.Z., C. Bergman, N.H. Patel, and M. Kreitman. 2000. Evidence for stabilizing selection in a eukaryotic enhancer element. *Nature* **403:** 564-567.

Margulies, E.H., M. Blanchette, D. Haussler, and E.D. Green. 2003. Identification and characterization of multi-species conserved sequences. *Genome Res* **13:** 2507-2518.

Margulies, E.H., J.P. Vinson, W. Miller, D.B. Jaffe, K. Lindblad-Toh, J.L. Chang, E.D. Green, E.S. Lander, J.C. Mullikin, and M. Clamp. 2005. An initial strategy for the systematic identification of functional elements in the human genome by low-redundancy comparative sequencing. *Proc Natl Acad Sci U S A* **102:** 4795-4800.

Nobrega, M.A., I. Ovcharenko, V. Afzal, and E.M. Rubin. 2003. Scanning human gene deserts for long-range enhancers. *Science* **302:** 413.

Oda-Ishii, I., V. Bertrand, I. Matsuo, P. Lemaire, and H. Saiga. 2005. Making very similar embryos with divergent genomes: conservation of regulatory mechanisms of Otx between the ascidians Halocynthia roretzi and Ciona intestinalis. *Development* **132:** 1663-1674.

Ovcharenko, I., L. Stubbs, and G.G. Loots. 2004. Interpreting mammalian evolution using Fugu genome comparisons. *Genomics* **84:** 890-895.

Pennacchio, L.A., N. Ahituv, A.M. Moses, S. Prabhakar, M. Nobrega, M. Shoukry, S. Minovitsky, I. Dubchak, A. Holt, K.D. Lewis, I. Plajzer-Frick, J. Akiyama, S. De Val, V. Afzal, B.L. Black, O. Couronne, M.B. Eisen, A. Visel and E.M. Rubin. 2006. *In vivo* enhancer analysis of human conserved noncoding sequences. *Nature*, in press.

Pennacchio, L.A. and E.M. Rubin. 2001. Genomic strategies to identify mammalian regulatory sequences. *Nat Rev Genet* **2:** 100-109.

Sandelin, A., P. Bailey, S. Bruce, P.G. Engstrom, J.M. Klos, W.W. Wasserman, J. Ericson, and B. Lenhard. 2004. Arrays of ultraconserved non-coding regions span the loci of key developmental genes in vertebrate genomes. *BMC Genomics* **5:** 99.

Stone, E.A., G.M. Cooper, and A. Sidow. 2005. Trade-offs in detecting evolutionarily constrained sequence by comparative genomics. *Annu Rev Genomics Hum Genet* **6:** 143-164.

Woolfe, A., M. Goodson, D.K. Goode, P. Snell, G.K. McEwen, T. Vavouri, S.F. Smith, P. North, H. Callaway, K. Kelly, K. Walter, I. Abnizova, W. Gilks, Y.J. Edwards, J.E. Cooke, and G. Elgar. 2005. Highly conserved non-coding sequences are associated with vertebrate development. *PLoS Biol* **3:** e7.

Website References

http://enhancer.lbl.gov/

http://genome.lbl.gov/vista

http://pipeline.lbl.gov

http://genome.ucsc.edu

http://jgi.doe.gov

Figure Legends

Figure 1. Whole-genome noncoding conservation and the funnel principle: correlation between ancient and recent noncoding conservation (funnel principle), illustrated by four Evolutionary Stacking Patterns (ESPs). HMR/G/X/F: human-mouse-rat/chicken/frog/fish. The four ESPs depict four sets of whole-genome HMR CNS, categorized by their most ancient overlapping non-mammalian CNS. Stacked below the rectangular blocks representing HMR CNSs are blocks depicting the corresponding ancient CNSs. (A) Category 1 CNSs extend to HMF, (B) Category 2 to HMX, (C) Category 3 to HMG and (D) Category 4 is limited to HMR. Block width is proportional to median CNS length in human, and block area is proportional to the median of -log(*P*-value). Block height thus represents degree of evolutionary constraint at the basepair level. Error bars mark the range from the 25th to the 75th percentile of CNS length. The funnel principle takes its name from the funnel-like shape of ESPs.

Figure 2. Whole-genome noncoding conservation and the funnel principle: strong enrichment for non-mammalian conservation in top-ranked (lowest-*P*-value) human-mouse-rat CNSs. (A) Cumulative fraction of non-mammalian CNSs overlapped by various quantiles of human-mouse-rat CNSs. The top 10% of human-rodent CNSs (by *P*-value) constitute a set of 17,185 sequences with a high degree of recent evolutionary conservation, that encompass 60% of whole-genome human-mouse-fish CNSs, 46% of human-mouse-frog CNSs and 30% of human-mouse-chicken CNSs. (B) The 171,853 human-rodent CNSs are binned by *P*-value. Vertical bars represent the fraction of

human-rodent CNSs in each bin that overlap more ancient CNSs.

Figure 3. *DACH1* locus: identification of long-range embryonic enhancers by extreme human-rodent CNSs with no conservation in fish. The Gumby human-mouse-rat conservation plot in the lower half of the figure depicts 784 CNSs (red vertical bars) in a 2-Mb genomic region containing the *DACH1* gene, many of which have extremely low *P*-values. Blue ticks below the line mark *DACH1* exons. Six of the human-rodent CNSs with *P*-value < 1e-50 and no conservation in fish were tested for enhancer activity at embryonic day 11.5-12.5; the resulting positives and negatives are marked by (+) and (-) symbols, respectively. The identified enhancers drove reproducible beta-galactosidase expression in limbs, eyes and brain, consistent with the endogenous expression domains of *DACH1*.

Figure 4. Extreme human-rodent CNSs with no conservation in fish identify enhancers at E11.5-12.5 only in certain genomic regions. Upper and lower plots: human-rodent (blue) and human-mouse-fish (scaled by a factor of 5, red) CNS density on the p (upper) and q (lower) arms of human chromosome 16. We tested 24 human-rodent CNSs with *P*-value < 1e-40 and no conservation in fish (locations marked by vertical lines) for enhancer activity at embryonic day 11.5-12.5. The 5 enhancers thus identified were located exclusively in two of the four loci with the highest human-mouse-fish CNS density on the chromosome (yellow bands). These loci contain developmentally regulated genes, all but one of which are transcription factors.

Figure 5. *SCL* locus: benchmarking eutherian sequence comparison against empirical data. The displayed 60-kb genomic region contains the *SCL* gene and its flanking intergenic regions. Human-mouse-rat-dog CNSs (red) and exonic (blue) conserved regions identified by Gumby (*P*-value ≤ 0.5) are shown as vertical bars. The 9 CNSs marked with asterisks identify 8/10 benchmark sequence elements with empirical evidence of *cis*-regulatory function (green rectangles). Additionally, there are 11 new predictions at this *P*-value threshold.

Figure 1

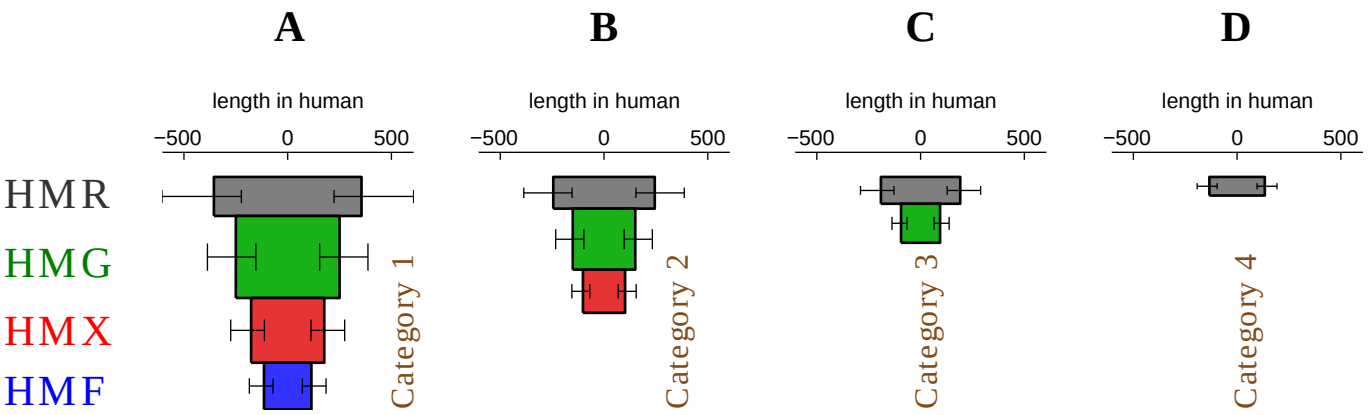
A
B
C
D
length in human
−500
0
500
HMR
HMG
HMX
HMF
Category 1
Category 2
Category 3
Category 4

Figure 2

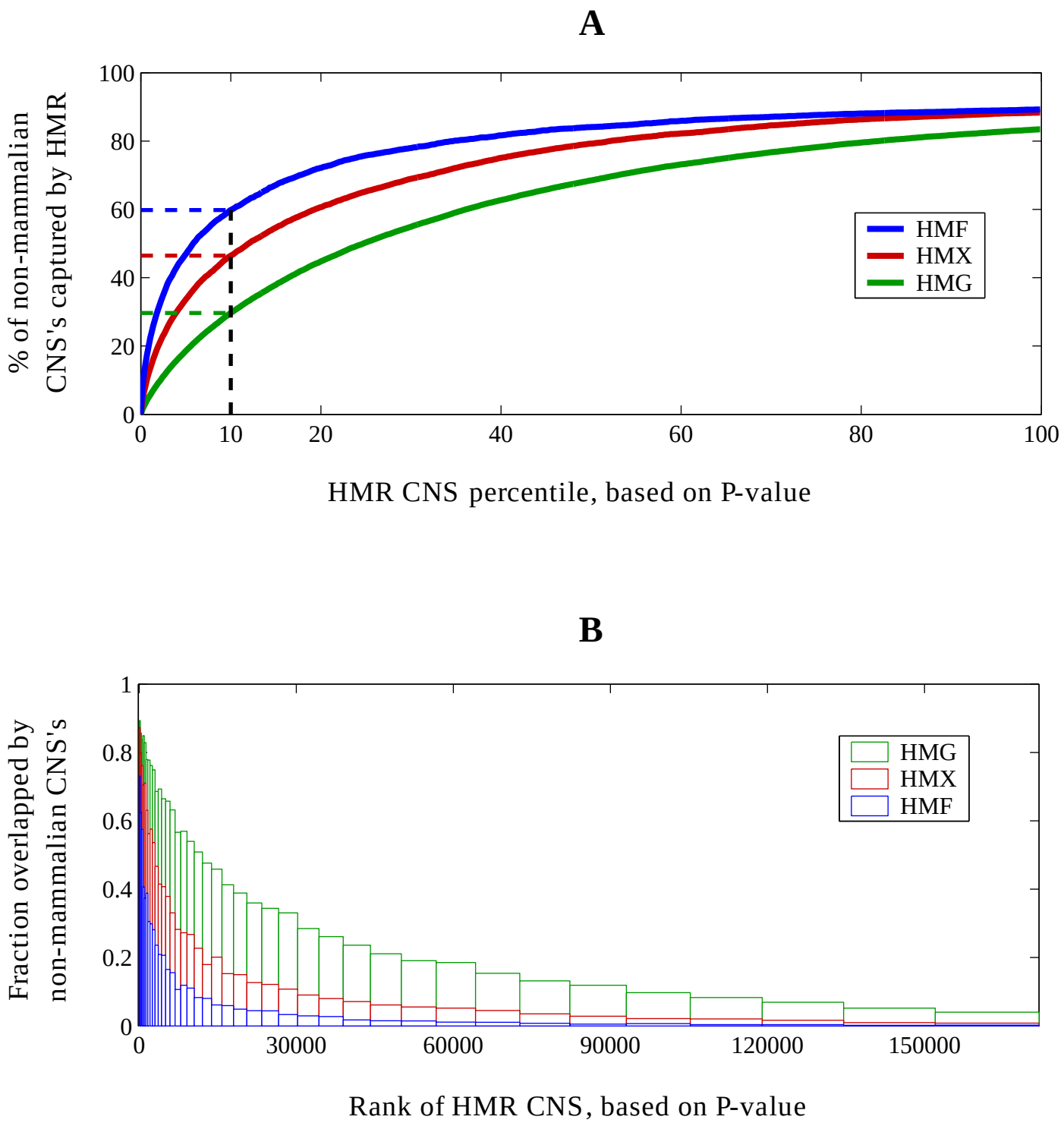
A
% of non-mammalian CNS's captured by HMR
100
80
60
40
20
0
0
10
20
40
60
80
100
HMF
HMX
HMG
HMR CNS percentile, based on P-value
B
Fraction overlapped by non-mammalian CNS's
1
0.8
0.6
0.4
0.2
0
0
30000
60000
90000
120000
150000
HMG
HMX
HMF
Rank of HMR CNS, based on P-value

Figure 3

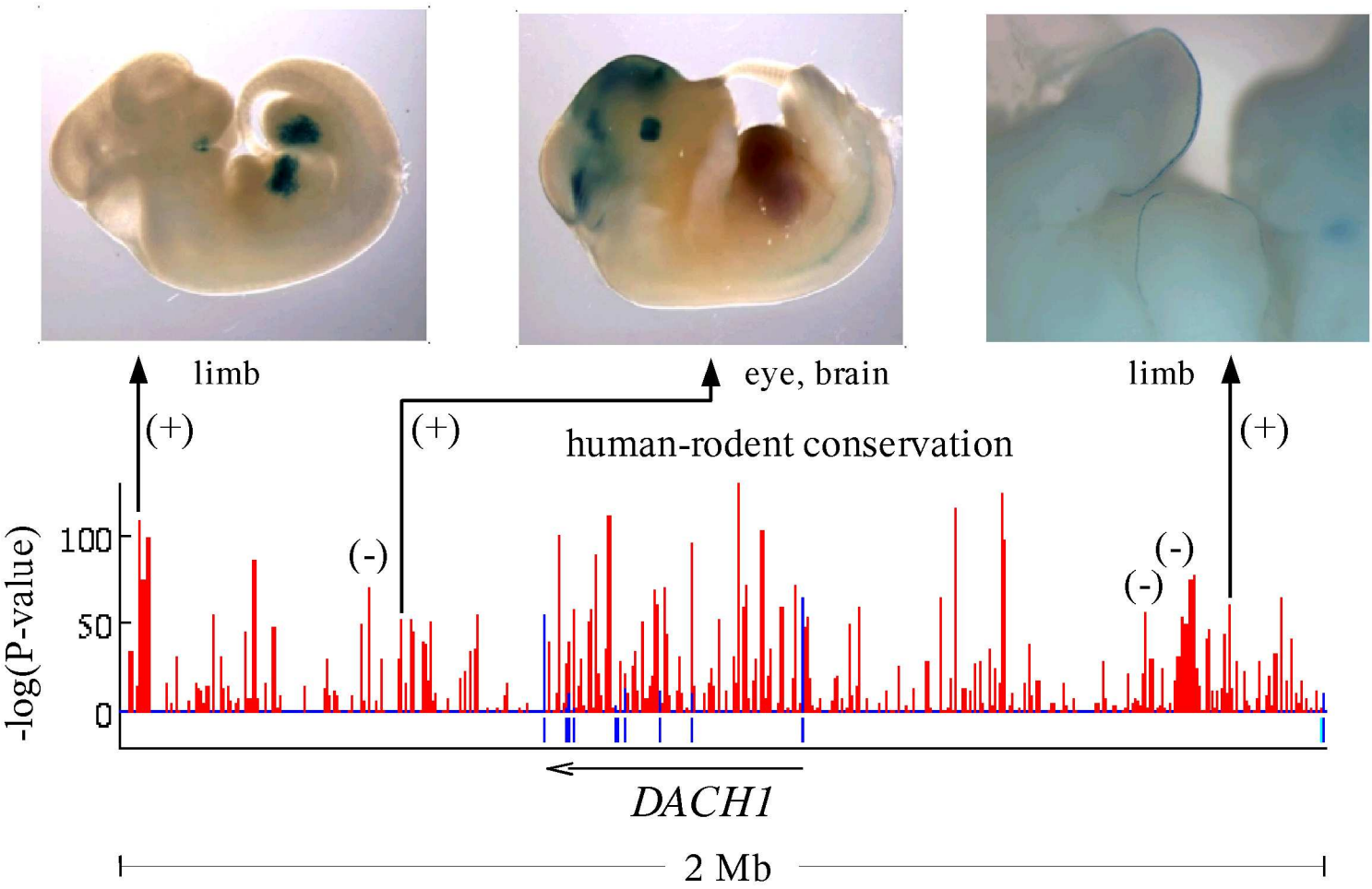
limb
eye, brain
limb
(+)
(+)
(+)
human-rodent conservation
(-)
(-)
(-)
100
50
0
-log(P-value)
DACH1
2 Mb

Figure 4

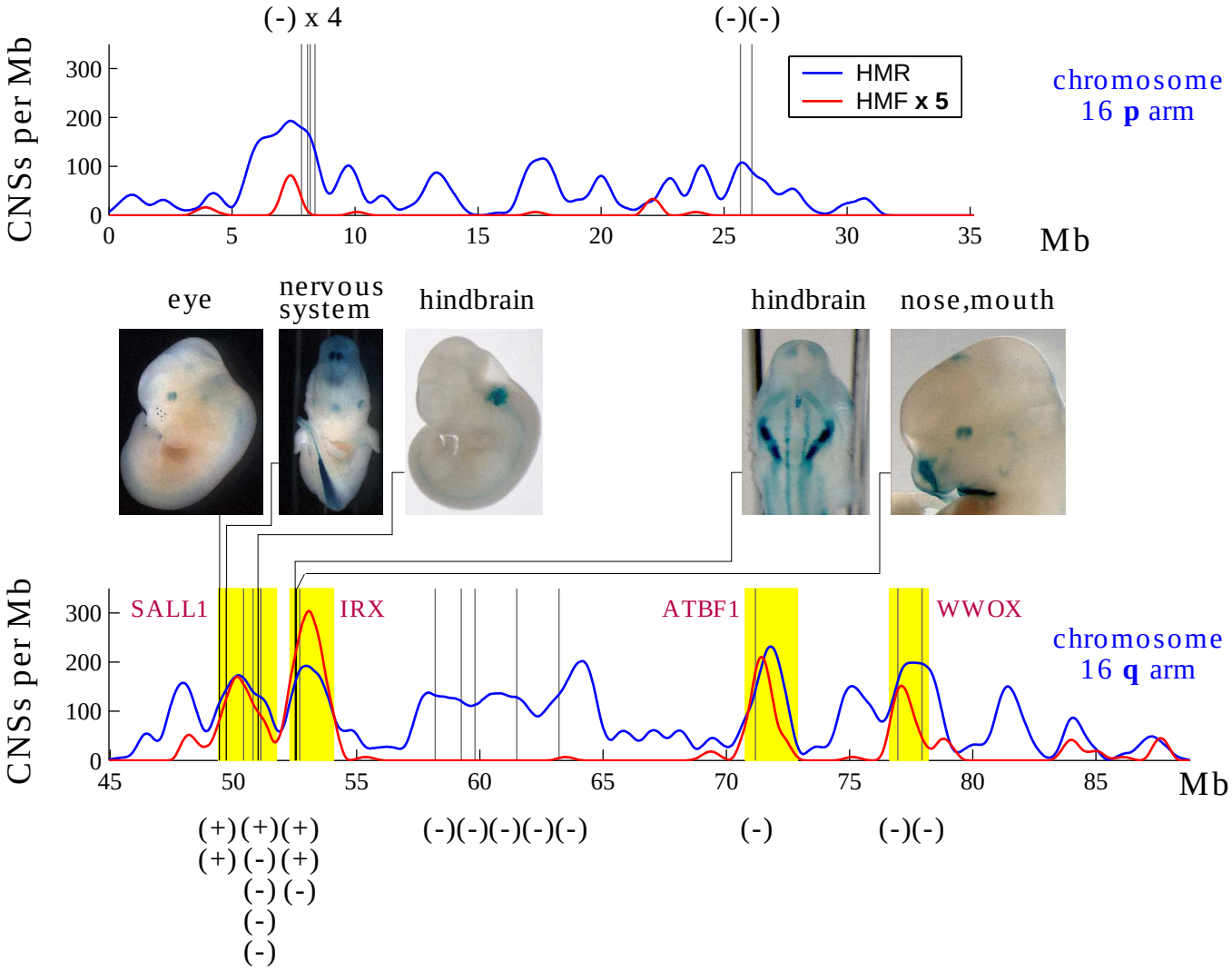
(-) x 4
(-)(-)
CNSs per Mb
300
200
100
0
0
5
10
15
20
25
30
35
Mb
HMR
HMF x 5
chromosome
16 p arm
eye
nervous
system
hindbrain
hindbrain
nose,mouth
SALL1
IRX
ATBF1
WWOX
chromosome
16 q arm
45
50
55
60
65
70
75
80
85
(+) (+)(+)
(+) (-) (+)
(-) (-)
(-)
(-)
(-)(-)(-)(-)(-)
(-)
(-)(-)

Figure 5

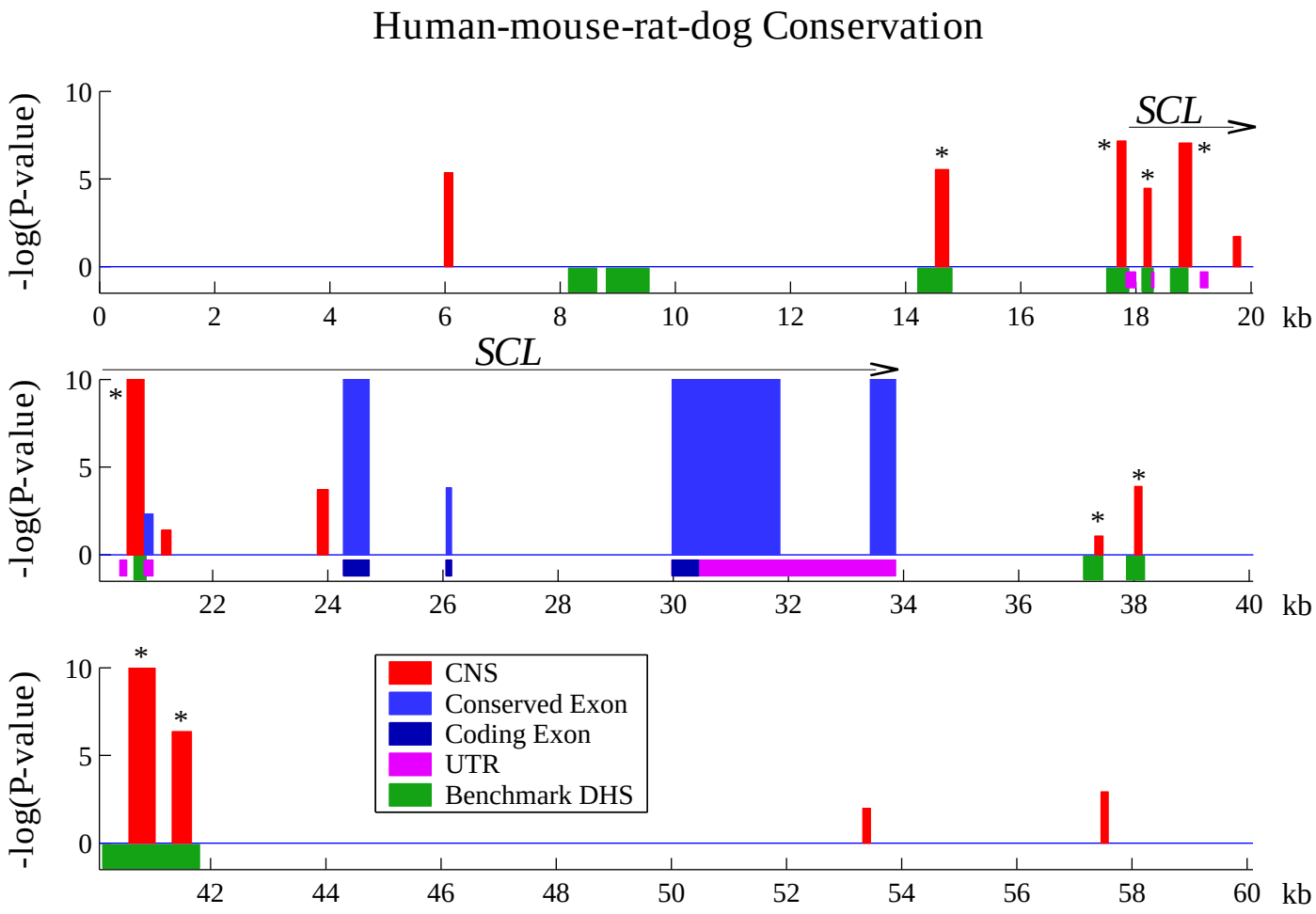
Human-mouse-rat-dog Conservation
-log(P-value)
SCL
kb
CNS
Conserved Exon
Coding Exon
UTR
Benchmark DHS

Supplementary Methods

Sources of Sequence Data and Genome Annotations

Most of the comparative analyses were performed with genomic sequences downloaded from the UCSC Genome Bioinformatics website (Kent et al. 2002) (http://genome.ucsc.edu). The following genome assemblies were used: the May 2004 human reference sequence, the May 2004 mouse genome assembly, the June 2003 rat genome assembly, the February 2004 chicken genome assembly, the June 2004 zebrafish genome assembly, the February 2004 tetraodon genome assembly and the August 2002 fugu genome assembly. Version 3.0 of the frog (*Xenopus tropicalis*) genome assembly was downloaded from the DoE Joint Genome Institute website (http://jgi.doe.gov). Gene, EST and mRNA annotations for these genome assemblies were obtained from the UCSC Genome Browser database (Karolchik et al. 2003). Multi-species sequence data from the alpha-globin locus were obtained as described in (Hughes et al. 2005).

Gumby self-training

Gumby's self-training step assumes that most nonexonic aligned positions evolve at the neutral rate. However, in the case of distantly related species pairs such as human-fugu, there are two reasons why this assumption is violated. Firstly, the fugu genome is compact, and the constrained fraction of the genome is therefore significantly large. Secondly, since the human-fugu evolutionary distance is well over 1 substitution/site,

global alignment programs tend to underestimate the neutral mismatch rate by identifying spurious homologies in neutral genomic regions. Although these two factors artificially lower Gumby's null-model mismatch rate, the effect is not as severe as one might expect, since the true mismatch rate saturates at ~0.74 mismatches/site (assuming 40% GC content), and the median human-fugu Gumby estimate in whole-genome noncoding alignments is 0.49 mismatches/site, which is significantly lower than the true value, but not so low as to render constrained regions invisible to Gumby. Another limitation of self-training is that Gumby cannot score sequence conservation in short alignments that contain very few aligned noncoding positions. Nevertheless, the self-training step is crucial to Gumby's ability to process alignments at all evolutionary distances without prior estimates of evolutionary parameters.

Potential artifacts from CNS edge errors and false-positive CNSs

We investigated the possibility of systematic errors in CNS edge detection, since artifactual lengthening of human-rodent CNSs or shortening of more deeply conserved CNSs by Gumby could potentially generate a funnel effect even in the absence of any genuine variation in the length of constrained noncoding sequences. Performance of Gumby in human-rodent analysis was tested by means of evolutionary simulations generated by the *simali* program (Blanchette et al. 2004). Each simulation started with a 20-kb ancestral mammalian sequence, which was neutrally propagated down the branches of the human-mouse-rat phylogenetic tree by means of point substitutions and indels, including insertion of transposable elements. The neutrally evolving 20-kb blocks

were preceded by indel-free constrained sequences of length 250 bp, evolving at half the neutral substitution rate. The edge error of each "true positive" human-mouse-rat CNS detected by Gumby was calculated as twice the difference in basepairs between the right edges of the constrained block and the Gumby prediction. The median edge error was 6 bp at a *P*-value threshold of 0.5, and 12 bp at 1e-3. These errors are too small to account for the 484-bp difference between median human-mouse-rat and human-mouse-fugu whole-genome CNS lengths.

The possibility of artifactual shortening of human-mouse-fugu CNSs by Gumby was examined using the 47 human-mouse-fugu CNSs (*P*-value <= 1e-3) detected by Gumby in the *DACH1* locus as a test case. These 47 CNSs span 22,878 bp of human DNA, and are covered by 38 human-mouse-rat CNSs (*P*-value <= 1e-3) spanning 65,489 bp. Within the human-mouse-fugu CNSs, 48.3% of human nucleotides are identical to the aligned fugu nucleotide, whereas only 15.2% are identical in the flanking regions that are outside the Gumby human-mouse-fugu prediction but inside the human-mouse-rat CNS. Thus, it is hard to imagine any criterion for sequence conservation that would extend the Gumby human-mouse-fugu CNSs to match human-mouse-rat CNSs in length.

It is conceivable that the weaker human-rodent CNSs show less conservation in distant species merely because they are mostly false positives, i.e. "noise," in which case the funnel principle would not be valid. However, even the weakest CNSs considered in this section have a *P*-value of at most 1e-3 in a 10-kb stretch of human DNA, at which threshold the expected false-positive rate is ~1 CNS per 10 Mb. Thus, only ~250 false

positives are expected in the ~2.5 Gb of syntenic blocks aligned between human, mouse and rat. Since the observed number of CNSs at this *P*-value threshold is larger by a factor of ~680, we do not expect any significant artifacts from false-positive CNSs. To further support this conclusion, we analysed sequence conservation in the aforementioned alignments of simulated neutrally evolving human, mouse and rat sequences. At a *P*-value threshold of 0.5, which corresponds to an *E*-value of 0.69 in 10 kb of human sequence, Gumby detected 0.35 conserved elements per 10 kb of neutrally evolving sequence, indicating that, at least in this simulation, Gumby *P*-value estimates are moderately conservative. Thus, it is highly unlikely that false-positive CNSs make any significant contribution to the whole-genome trends encapsulated in the funnel principle.

Analysis of *SCL* and alpha-globin loci

Sequence alignment and estimation of substitution rates

Sequence alignment and comparative analysis of primate and more distant genomes at the alpha-globin locus presented a particular challenge, due to the high frequency of lineage-specific tandem duplications and gene conversion events among the globin genes and pseudogenes, and the incompleteness of primate, cat, cow and pig sequence data. In order to minimize artifacts of misalignment and missing sequence data, we split the alpha-globin region into 4 sub-regions (human chromosome 16: 48,339-76,733, 76,704-144,429, 155,156-171,107 and 171,108-219,839), and aligned each one of them separately using MLAGAN. In each sub-region, we excluded from the analysis species with long stretches of missing sequence data. Thus, we excluded dusky titi in the first

sub-region, colobus and cat in the third sub-region, and baboon, colobus, squirrel monkey and cat in the fourth sub-region. In addition, we excluded mouse in the fourth sub-region, due to lack of synteny. Multiple alignments of the third sub-region were curated by hand to avoid misalignments between the tandemly duplicated globin genes.

We used the program fastDNAml (Olsen et al. 1994) to estimate neutral substitution rates in the alpha-globin and *SCL* loci. Estimates were based on fastDNAml analysis of the entire multiple sequence alignment, rather than noncoding regions alone. However, since coding exons constitute only a small fraction of the analyzed genomes, we do not expect their inclusion to introduce significant biases in rate estimates. Estimates of substitution rates in the alpha-globin locus were performed separately in each of the four aligned sub-regions, due to variation in the species set across sub-regions.

Estimation of sensitivity and false-positive rate

A benchmark set of 10 sequence elements in the *SCL* locus with evidence of cis-regulatory function was derived from (Chapman et al. 2004), after exclusion of a DHS that overlaps a coding exon of *SCL*. Similarly, the 17 benchmark sequence elements in the alpha-globin locus were derived from (Hughes et al. 2005), after elimination of 4 alternatively spliced exons and 3 unclassified sequence elements. In evaluating the accuracy of comparative sequence analysis at these loci, a benchmark sequence element was considered to be identified by a CNS if there was any overlap (even 1 bp is sufficient) between the two. CNSs not overlapping benchmark elements were classified as new predictions. An exception was made in the case of conserved elements in the

alpha-globin locus overlapping the 4 previously unannotated alternate exons identified in (Hughes et al. 2005). These conserved elements were classified neither as true positives nor as new predictions; instead they were filtered out of the list of computational predictions before comparison to the benchmark.

An alternative approach to that used here would be to define sensitivity and specificity at the level of individual basepairs. However we are unable to employ such a strategy, since, to the best of our knowledge, the precise boundaries are not known of any of the benchmark functional elements used in this study.

Cloning

Enhancer element constructs were PCR amplified from human genomic DNA (BD Biosciences) and directionally cloned into the pENTR/D-TOPO vector (Invitrogen). All constructs were sequenced and transferred to the Gateway-HSP68-LacZ vector using the LR recombination reaction (Invitrogen).

Generation of transgenic mice

Plasmid DNA was purified using the EndoFree plasmid maxi kit (Qiagen). 100 μg of plasmid was linearized with XhoI, followed by purification on Micropure EZ columns and Montage PCR filter units (Millipore). The purified DNA was dialyzed 24h against injection buffer (10 mM Tris, pH 7.5; 0.1 mM EDTA), and its concentration determined

fluorometrically and by agarose gel electrophoresis. The DNA was diluted to a concentration of 1.5 to 2 ng/l and used for pronuclear injections of FVB embryos in accordance with protocols approved by the Lawrence Berkeley National Laboratory.

Embryo staining

Embryos were harvested at 11.5-12.5 dpc and dissected in cold 100mM phosphate buffer pH 7.3, followed by 30 min. of incubation with 4% paraformaldehyde at 4 ºC. The embryos' heads were punctured with a 27 g needle to facilitate the penetration of the staining solution and washed three times 30 min. with wash buffer (2 mM MgCl2; 0.01% deoxycholate; 0.02% NP-40; 100 mM phosphate buffer, pH 7.3). Embryos were stained for 24 h at room temperature with freshly made staining solution (0.8 mg/ml X-gal; 4 mM potassium ferrocyanide; 4 mM potassium ferricyanide; 20 mM Tris, pH 7.5 in wash buffer). Stained embryos were rinsed 3 times in 100 mM phosphate buffer pH 7.3, and post-fixed in 4% paraformaldehyde. Yolk sacs were carefully dissected from embryos and DNA was prepared by boiling the tissue for 20 min in 75 l of solution 1 (25 mM NaOH; 0.2 mM EDTA), followed by neutralization with 75 l of solution 2 (40 mM Tris-HCl). Yolk sac DNA was screened by PCR with LacZ primers (LacZ-fwd 5'-TTTCCATGTTGCCACTCGC; LacZ-Rev 5'-AACGGCTTGCCGTTCAGCA).

References

Blanchette, M., W.J. Kent, C. Riemer, L. Elnitski, A.F. Smit, K.M. Roskin, R. Baertsch, K. Rosenbloom, H. Clawson, E.D. Green, D. Haussler, and W. Miller. 2004. Aligning multiple genomic sequences with the threaded blockset aligner. *Genome Res* **14:** 708-715.

Karolchik, D., R. Baertsch, M. Diekhans, T.S. Furey, A. Hinrichs, Y.T. Lu, K.M. Roskin, M. Schwartz, C.W. Sugnet, D.J. Thomas, R.J. Weber, D. Haussler, and W.J. Kent. 2003. The UCSC Genome Browser Database. *Nucleic Acids Res* **31:** 51-54.

Kent, W.J., C.W. Sugnet, T.S. Furey, K.M. Roskin, T.H. Pringle, A.M. Zahler, and D. Haussler. 2002. The human genome browser at UCSC. *Genome Res* **12:** 996-1006.

Olsen, G.J., H. Matsuda, R. Hagstrom, and R. Overbeek. 1994. fastDNAmL: a tool for construction of phylogenetic trees of DNA sequences using maximum likelihood. *Comput Appl Biosci* **10:** 41-48.

Supplementary Figure 1. *SCL* locus: Sensitivity and true-positive rate of Gumby analysis of human-mouse-rat-dog sequence alignment at various values of the *R*-ratio, as the *P*-value threshold is varied from 0.5 to 1e-15.

Supplementary Figure 1

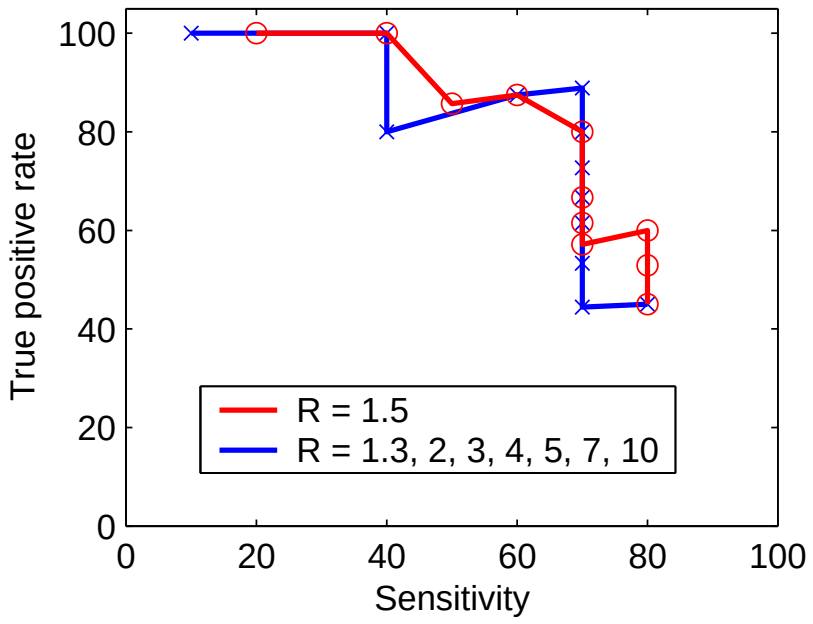

Supplementary Figure 2. In order to avoid the biases of sum-of-pairs and consensus schemes for scoring multiple alignments, Gumby scores each aligned position by summing pair-wise log-odds along a circular tour of the tree. Each species is considered twice in a circular tour, once with its clockwise neighbor, and once with its anti-clockwise neighbor.

Supplementary Figure 2

$$\boldsymbol{S} = S(H,M) + S(M,C) + S(C,D) + S(D,L) + S(L,H)$$